

# ELECTRICALLY CONDUCTING COMPOSITE HOLLOW FIBERS

Shi Hyeong Kim, Min Kyoon Shin, Seon Jeong Kim\*

Center for Bio-Artificial Muscle, Dept. of Biomedical Engineering, Hanyang University,  
Seoul, South Korea

\* Corresponding author([sjk@hanyang.ac.kr](mailto:sjk@hanyang.ac.kr))

**Keywords:** *conducting polymer, hollow fiber, coaxial electrospinning*

## Abstract

We have fabricated electrically conducting composite hollow fibers (HFs) using coaxial electrospinning and chemical polymerization. Randomly oriented and well aligned polyamic acid (PAA) HFs were successfully fabricated as templates with high surface area to volume ratio employing coaxial electrospinning. PAA HFs were converted to polyimide (PI) HFs through thermal treatment. Inner and outer surfaces of well aligned PI HF bundles were uniformly coated with a polyaniline conducting polymer by in situ chemical polymerization. These composite HF bundles had an electrical conductivity of 11.5 S/m. The average values of outer and inner diameters of the conducting HFs were 1005 and 815 nm, respectively. The conducting HF bundles are applicable as supercapacitors and actuators.

## 1. Introduction

Conducting polymers have been researched for applications in actuators, sensors, and energy storage devices because they have important properties, such as facile interconversion between redox states, high electrical conductivity, and good chemical stability [1–3]. Polyaniline (PANi) has many advantages when used in supercapacitor devices: electroactivity, a high doping level, excellent stability, a high specific capacitance, environmental stability, and controllable electrical conductivity [4]. For effective applications of conducting polymers, it is required to enhance the charge/discharge rate of the counter ion on the surface of the conducting polymer to obtain a charge balance in the electrolyte during the electrochemical reactions [5].

Conducting polymers with tubular structure are effective in enhancing the charge/discharge rate and capacity [6, 7]. The inside of a hollow tube can be also modified with other materials to further enhance its functionality [8].

Coaxial electrospinning is a versatile technique for novel tubular structures with well-controlled inner and outer sizes, morphologies and compositions [9]. Its concept is similar to that of the conventional electrospinning except for the use of coaxial capillary tips [9]. When the polymer solutions ejected from a syringe are charged using high voltage, the charge accumulation occurs on the surface of the sheath liquid coming out of the outer coaxial capillary. The pendant droplet of the sheath solution forms a conical shape due to the charge-charge repulsion induced by initial application of electric potential. The stresses generated in the sheath solution cause the core liquid to deform into the conical shape and then a compound coaxial jet is formed. Once the charge accumulation reaches a certain threshold value overcoming surface tension due to the increased applied potential, a fine jet extends from the cone, resulting in forming nanofibers in core-sheath configuration. By removing core materials, nano or microscale tubular structures are fabricated [9, 10].

In this work, we have made randomly oriented and aligned polyamic acid (PAA) HFs. Through thermal treatment, PAA HFs were converted to polyimide (PI) HFs because PI has excellent thermal and chemical stabilities, high mechanical strength, and good dielectric properties. Finally we have fabricated electrically conducting HFs coated with PANi by in situ chemical polymerization.

## 2. Experimental

### 2.1 Materials

The 1,2,4,5-benzenetetracarboxylic dianhydride (BTCD), 4,4'-oxydianiline (ODA), aniline, tetrahydrofuran (THF), methanol, dimethylformamide (DMF), heavy mineral oil, and ammonium persulfate used were purchased from Sigma Chemicals (USA).

### 2.2 Sample Preparation

### 2.2.1 Polyamic Acid Copolymerization

Polyamic acid as a polyimide precursor was synthesized by copolymerization of BTCD and ODA in a mixed THF/methanol (8:2) solution. The process consisted of initially adding the BTCD to the mixed solution and checking that complete dissolution had occurred, and then mixing the solution with an equimolar amount of ODA at room temperature [11].

### 2.2.2 Fabrication of Polyamic Acid Hollow Fibers

By using a coaxial electrospinning method, hollow fibers were fabricated from a 15 wt% solution of PAA. A high-voltage 15 kV (1 kV/cm) power supply was applied between the metallic sheath tip and the collector positioned across the gap (1 cm) between a pair of conical copper electrodes. The solution feed flow rate used was in the range 1–6  $\mu\text{l}/\text{min}$  in the core and 25  $\mu\text{l}/\text{min}$  in the sheath at room temperature. To fabricate the PAA HF, the PAA/mineral oil HF was immersed in octane for 12 h to extract the mineral oil.

### 2.2.3 Imidization

PAA was converted into PI via a stepwise heating treatment under flowing air at 40  $^{\circ}\text{C}$  for 4 h, 100  $^{\circ}\text{C}$  for 1 h, and 250  $^{\circ}\text{C}$  for 12 h. The heating rate was 5  $^{\circ}\text{C}/\text{min}$  [11].

### 2.2.4 Polymerization

The in situ polymerization of PI HF occurred after immersion in a 1 M HCl solution that contained 0.01 mol of aniline for 2 h, and then 0.0125 mol of ammonium persulfate was added to the solution and allowed to react for 24 h [12].

## 2.3 Characterization

The morphology of PANi-coated polyimide PI HF bundles was examined using field emission scanning electron microscopy (FE-SEM, Model S4800, Hitachi, Japan) under an accelerator voltage of 15 kV. Changes in the functional groups during imidization were characterized using Fourier transform infrared spectroscopy (FT-IR) (Infinity Gold FTIR 60AR, USA). The electrical conductivity based on a tow point probe method was measured using a Keithley electrometer (Model 2400, USA) at room temperature.

## 3. Results and Discussion

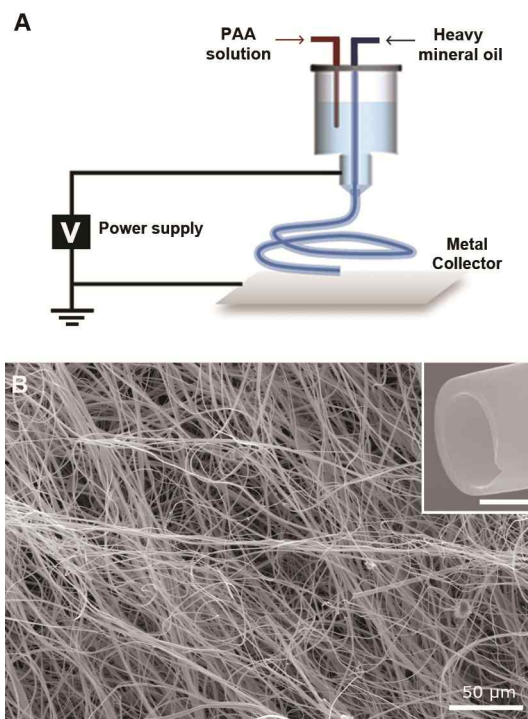


Fig. 1. (A) A schematic illustration of the setup used to obtain HF with electrospinning. The spinneret consisted of inner and outer needles, through which heavy mineral oil and PAA were simultaneously emitted to form a coaxial jet. (B) An SEM image of the PAA HF. The inset image shows a cross-section of a PAA HF. (scale bar: 1  $\mu\text{m}$ )

Figure 1A shows a schematic drawing of the setup used for the coaxial electrospinning to fabricate the HF. This is similar to conventional electrospinning, except for the use of metallic coaxial capillary tips. The coaxial tips consist of an 18G metallic needle as a sheath and a 26G metallic needle as a core to emit a solution from the needle sheath and core at the same time.

A 15 wt% PAA solution was prepared by copolymerizing BTCD and ODA in a THF and methanol mixed solvent. The PAA solution was electrospun into PAA HF. In the procedure to fabricate PAA HF, both the PAA solution as the sheath material and the mineral oil as the core material were simultaneously fed using a syringe pump. The feed rate used was 4  $\mu\text{l}/\text{min}$  in the core and 25  $\mu\text{l}/\text{min}$  in the sheath. When a voltage of 15 kV was applied between the metallic sheath tip and the collector, the compound liquid was deformed into a Taylor cone, and a coaxial jet was formed. The coaxial jet was stretched by the electrostatic force. The rapid stretching of the sheath of the coaxial jet caused strong viscous stress (shear

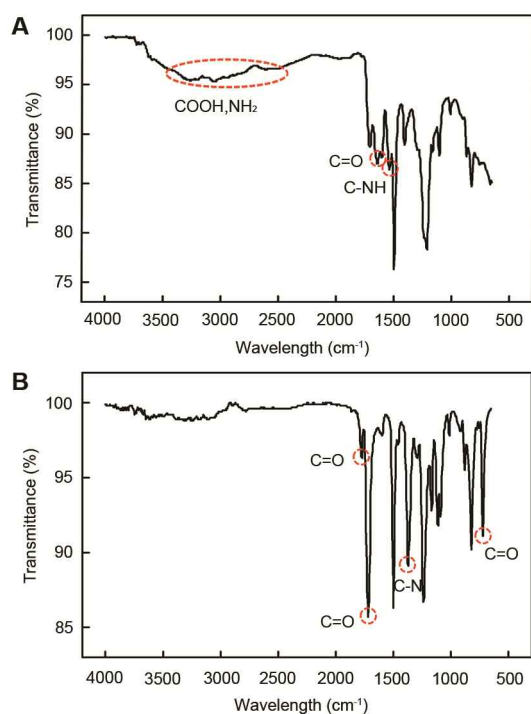


Fig. 2. Fabrication of PAA and PAA converted into PI. The FT-IR spectra show: (A) PAA and (B) PI.

stress, contact friction), which dragged the mineral oil along with the PAA solution, resulting in the formation of a coaxial fiber [10]. The coaxial fibers were immersed in octane for 12 h to extract the mineral oil, resulting in the fabrication of the randomly oriented and long PAA HF (Figure 1B). The outer diameter of PAA HF ranged from 2 to 3  $\mu\text{m}$  and the wall thickness ranged from 300 to 500 nm. The inset image in Figure 1B shows a cross section of a PAA HF.

After fabricating the PAA HF, we checked evidence of the formation of PAA HF in their FT-IR spectra. Figure 2A shows the FT-IR spectrum of PAA HF showing peaks associated with  $\text{NH}_2$  and  $\text{COOH}$ ,  $\text{C}=\text{O}$ , and  $\text{C}-\text{NH}$  indicated by the broad absorption occurring between  $2500\text{ cm}^{-1}$  and  $3500\text{ cm}^{-1}$ , at  $1646.2\text{ cm}^{-1}$ , and at  $1540.5\text{ cm}^{-1}$ , respectively. We converted the PAA HF into PI HF through a stepwise thermal treatment process for solvent removal and imidization of the PAA tubes (under ambient conditions at  $40\text{ }^\circ\text{C}$  for 4 h,  $100\text{ }^\circ\text{C}$  for 1 h, and  $250\text{ }^\circ\text{C}$  for 12 h).

Figure 2B shows the FT-IR spectrum of the PI HF showing a peak from the  $\text{C}=\text{O}$  symmetric stretch at  $1780\text{ cm}^{-1}$ , the  $\text{C}=\text{O}$  asymmetric stretch at  $1725\text{ cm}^{-1}$ ,  $\text{C}-\text{N}$  at  $1376\text{ cm}^{-1}$ , and  $\text{C}=\text{O}$  bonding at  $725\text{ cm}^{-1}$  [13]. Because the PI HF has superior properties, including chemical durability, thermal

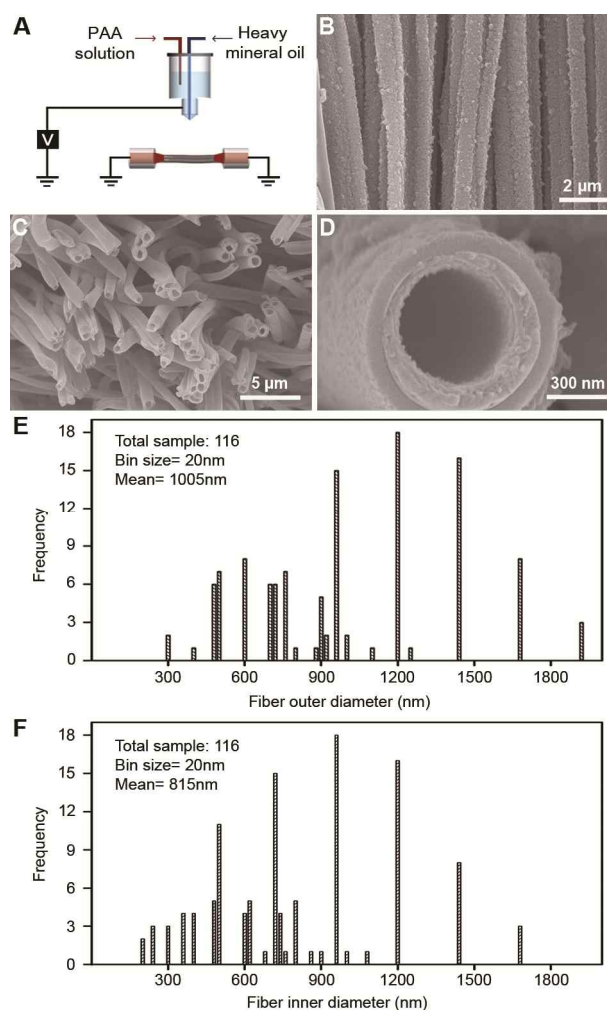


Fig. 3. (A) A schematic illustration of the setup used for HF. The collector consisted of two electrodes across the gap between a pair of conical copper electrodes. (B) PANi-coated aligned PI HF. (C) A cross-sectional image of PANi-coated aligned PI HF bundles. (D) The PANi-coated inner and outer surfaces of a hollow structure. PI HF bundle distribution diameters of (E) the outer and (F) inner surfaces.

stability, and high surface area to volume ratio, they provide a suitable template for coating conducting polymers.

For effective coating of conducting polymers during in situ polymerization, we controlled the alignment and the diameter of the PI HF. Figure 3A shows the setup used to make aligned HF bundles. To obtain well-aligned HF bundles we used a collector across the gap between a pair of conical copper electrodes instead of a rectangular metal collector [14]. During electrospinning, the charged coaxial fiber should experience two different electrostatic forces—the applied electric field and the Coulomb interactions between the charged

coaxial fiber and the collector—so that the coaxial fibers form efficiently stretched, perpendicularly suspended bundles in the gap on the collector [14].

Figures 3B and 3C show well-aligned and uniform PI HF bundles coated with PANi. We observed that different thicknesses of the PANi inner coating are obtained for the different inner diameters of the HFs. This result is related to changes in the capillary and diffusive forces between the PI HF and the aniline monomer dispersed in the solution. We used two methods to control the inner diameter. First, by modulating the amount of DMF from 1 to 10 v/v% to increase the ionic conductivity of the electrospinning solution [15], PI HFs with inner diameters ranging from 1  $\mu\text{m}$  to 100 nm were fabricated, respectively. Second, by controlling the feed rate of the core solution from 1 to 6  $\mu\text{l}/\text{min}$ , PI HFs with inner diameters varying from 250 to 400 nm were obtained. When the inner diameter of the PI HFs was  $> 700$  nm, the aniline monomer entered the HFs due to the capillary and diffusive forces, resulting in a coating of both the inner and outer walls of the PI HFs, as shown in Figure 3D [16].

Figures 3E and 3F show the distribution of the fiber diameters for both the outer and inner surfaces when a voltage of 15 kV (1 kV/cm) was applied between the metallic sheath tip and the collector. The feed rate of the PAA solution with 5v/v% DMF was 6  $\mu\text{l}/\text{min}$  in the core and 25  $\mu\text{l}/\text{min}$  in the sheath at room temperature. The fiber diameter distribution of conducting HFs was determined from 116 HFs. The average values of outer and inner diameters of the conducting HFs were 1005 and 815 nm, respectively. These PANi-coated PI HFBs had an electrical conductivity of 11.5 S/m.

#### 4. Conclusions

We successfully fabricated PANi-coated PI HFBs using coaxial electrospinning. Our study should open the way for the use of both the inner and outer surfaces of HFs. PANi coating on the inner and outer surfaces of PI HFBs will enhance the efficiency of the charge/discharge process and the capacitance. Therefore, this structure has potential applications in supercapacitors and artificial muscles.

#### Acknowledgements

This work was supported by the Creative Research Initiative Center for Bio-Artificial Muscle of the Ministry of Education, Science & Technology (MEST) in Korea.

#### References

- [1] G. A. Snook, P. Kao and A. S. Best “Conducting-polymer-based supercapacitor devices and electrodes”. *Journal of Power Sources*, Vol. 196, No. 1, pp 1-12, 2011.
- [2] R. H. Baughman “Conducting polymer artificial muscles”. *Synthetic Metals*, Vol. 78, No. 3. pp 339-353, 1996.
- [3] A. Rudge, J. Davey, I. Raistrick, S. Gottesfeld and J. P. Ferraris “Conducting polymers as active materials in electrochemical capacitors”. *Journal of Power Sources*, Vol. 47, No. 1-2, pp 89-107, 1994.
- [4] V. Gupta and N. Miura “High performance electrochemical supercapacitor from electrochemically synthesized nanostructured polyaniline”. *Materials Letters*, Vol. 60, No. 12, pp 1466-1469, 2006.
- [5] Y. Wang, H. Li and Y. Xia “Ordered whiskerlike polyaniline grown on the surface of mesoporous carbon and its electrochemical capacitance”. *Advanced Materials*, Vol. 18, No. 19, pp 2619-2623, 2006.
- [6] S. Cho and S. B. Lee “Fast Electrochemistry of Conductive Polymer Nanotubes: Synthesis, Mechanism, and Application” *ACCOUNTS OF CHEMICAL RESEARCH*, Vol. 41, No. 6, pp 699-707, 2008.
- [7] P. Simon and Y. Gogotsi “Materials for electrochemical capacitors” *nature materials*, Vol. 7, No. 11, pp 845-854, 2008.
- [8] D. Li, J. T. McCann and Y. Xia “Use of electrospinning to directly fabricate hollow nanofibers with functionalized inner and outer surfaces”. *Small*, Vol. 1, No. 1, pp 83-86, 2005.
- [9] D. Li and Y. Xia “Electrospinning of nanofibers: reinventing the wheel?”. *Advanced Materials*, Vol. 16, No. 14, pp 1151-1170, 2004.
- [10] D. Li and Y. Xia “Direct fabrication of composite and ceramic hollow nanofibers by electrospinning”. *Nano Letters*, Vol. 4, No. 5, pp 933-938, 2004.
- [11] K. S. Yanga, D. D. Edie, D.Y. Lim, Y. M. Kim and Y. O. Choi “Preparation of carbon fiber web from electrostatic spinning of PMDA-ODA poly(amic acid) solution”. *Carbon*, Vol. 41, No. 11, pp 2039-2046, 2003.
- [12] Y. A. Ismail, S. R. Shin, K. M. Shin, S. G. Yoon, K. Shon, S. I. Kim and S. J. Kim “Electrochemical actuation in chitosan/polyaniline microfibers for artificial muscles fabricated using an in situ polymerization”. *Sensors and Actuators B*, Vol. 129, No. 2, pp 834-840, 2008.
- [13] C. Nah, S. H. Han, M.-H. Lee, J. S. Kim and D. S. Lee “Characteristics of polyimide ultrafine fibers prepared through electrospinning”. *Polymer International*, Vol. 52, No. 3, pp 429-432, 2003.
- [14] W. E. Teo and S. Ramakrishna “Electrospun fibre bundle made of aligned nanofibres over two fixed points”. *Nanotechnology*, Vol. 16, No. 9, pp 1878-1884, 2005.
- [15] T. Uyar and F. Besenbacher “Electrospinning of uniform polystyrene fibers: The effect of solvent conductivity”. *Polymer*, Vol. 49, No. 24, pp 5536-5543, 2008.
- [16] K. Jayaraman, K. Okamoto, S. J. Son, C. Luckett, A. H. Gopalani, S. B. Lee and D. S. English “Observing capillarity in hydrophobic silica nanotubes”. *Journal of the American Chemical Society*, Vol. 127, No. 49, pp 17385-17392, 2005.